



N. Katebi  
E. Kolpakova-Hart  
C. Y. Lin  
B. R. Olsen

## The mouse palate and its cellular responses to midpalatal suture expansion forces

### Authors' affiliation:

N. Katebi, E. Kolpakova-Hart, C. Y. Lin,  
B. R. Olsen, Department of Developmental  
Biology, Harvard School of Dental Medicine,  
Boston, MA, USA

### Correspondence to:

Bjorn R. Olsen  
Department of Developmental Biology  
Harvard School of Dental Medicine  
188 Longwood Avenue  
Boston, MA 02115  
USA  
E-mail: bjorn\_olsen@hms.harvard.edu

Katebi N., Kolpakova-Hart E., Lin C. Y., Olsen B. R. The mouse palate and its cellular responses to midpalatal suture expansion forces

*Orthod Craniofac Res* 2012;15:148–158. © 2012 John Wiley & Sons A/S

### Structured Abstract

**Objectives** – To investigate the anatomy of the mouse palate, the midpalatal suture, and the cellular characteristics in the sutures before and immediately after midpalatal suture expansion.

**Materials and Methods** – Wild-type C57BL/6 male mice, aged between 6 weeks and 12 months, were chosen for all the experiments. The complete palate of the non-operated group and the midpalatal suture-expanded group at different ages was used for histological, micro-CT, immunohistochemistry, and sutural cell analyses.

**Results** – This study documents precise morphological and histological characteristics of the mouse palatal sutures. In addition to the opening of the midpalatal suture caused by expansion, both transverse and interpalatine sutures were also seen to be affected. Cellular density was decreased in different types of sutures following the application of mechanical force.

**Conclusions** – The detailed morphology and histology of the mouse palate and the cellular changes that occur following midpalatal suture expansion, as described here, will be helpful as a basis for further investigations of palatal suture tissue responses to mechanical force.

**Key words:** collagen II; craniofacial sutures; mechanical force; mesenchymal cell; palate

## Introduction

Craniofacial sutures and synchondroses are flexible and less stiff than bones. Sutures are dynamic and respond to different types of mechanical stimuli (1). Taking advantage of these properties, orthopedic–orthodontic therapy utilizes applied mechanical stresses to stimulate or inhibit bone growth or to modify the direction of growth via changing cellular activities within craniofacial sutures and synchondroses (2).

Understanding the mechanisms by which craniofacial sutures respond to mechanical force is essential for improving orthodontic

### Date:

Accepted 7 May 2012

DOI: 10.1111/j.1601-6343.2012.01547.x

© 2012 John Wiley & Sons A/S

treatment strategies. Accordingly, scientists are increasingly interested in delineating the events that occur at the cellular and molecular levels during the application of mechanical forces across craniofacial sutures. For half a century, the expansion of one such suture, the midpalatal suture, has been successfully used to correct dentofacial deformities and treat maxillary width deficiencies (3). To obtain insights into the basic mechanisms involved, scientists have turned to midpalatal suture expansion in rats and mice. Because of their utility in uncovering genetic mechanisms, mice represent an ideal model for studying the responses of mammalian craniofacial bones and sutures to mechanical forces, and our laboratory has described how an expansive force across the mouse midpalatal suture induces a process of remodeling and regeneration of the suture structure (4). However, further studies of detailed molecular mechanisms require precise morphological and histological data on the mouse midpalatal suture that are currently unavailable. Thus, to provide such data, we have investigated the anatomy of the mouse palate, the midpalatal suture, and the cellular characteristics in the suture before and immediately after midpalatal suture expansion.

## Materials and methods

### Experimental animals and histological/micro-CT analyses of hard palate

Wild-type C57BL/6 male mice (Charles River Laboratories, Wilmington, MA, USA), aged between 6 weeks and 12 months, were used for all the experiments. Each experimental group consisted of a minimum of four mice. The whole palate of each mouse was dissected and fixed overnight with 4% (w/v) paraformaldehyde in 0.1 M phosphate buffer, pH 7.4, demineralized in 0.5 M ethylenediaminetetraacetic acid (EDTA) for 2 weeks at 4°C, and dehydrated in ethanol prior to embedding in paraffin. For histological analysis, 8- $\mu$ m serial paraffin sections of 6-week-old, 4-, 9-, and 12-month-old mice were cut. Microphotographs were taken (Nikon Eclipse 80i Upright Microscope; Nikon Corporation, Tokyo Japan) after sections were mounted on the glass slides,

de-waxed, and stained with hematoxylin and eosin. To obtain three- and two-dimensional views of the whole palate, tissues were subjected to high-resolution micro-CT analysis (Xradia MicroXCT system, Pleasanton CA, USA). The 3D viewing software provided with the Xradia scanner was used to generate the images. All animal work was performed using protocols approved by the Institutional Animal Care and Use Committee of Harvard Medical School, Boston, MA, USA.

### Midpalatal suture expansion procedure

A combination of ketamine (100 mg/kg) and xylazine (10 mg/kg) was used as anesthetic for the mice. The mice were prepared for midpalatal suture expansion as previously described. (4). Briefly, 0.014-in. stainless steel orthodontic wire (GAC International Inc., Bohemia, NY, USA) was used to make opening loops that applied a distracting force across the midpalatal suture. Using a light-cured adhesive (3 M Unitek, Monrovia, CA, USA), the appliances were bonded to first and second maxillary molars on both sides. For sham operation, dead opening loops with no expansion force were prepared and bonded to first and second maxillary molars. Mice were sacrificed after 2 days of midpalatal suture expansion, and the maxilla was dissected.

### Cell density in hard palate sutures

Hematoxylin- and eosin-stained palates of 6-week-old mice were analyzed for differences in cell density within palatal sutures. Using METAMORPH software (Molecular devices LLC; Sunnyvale, CA, USA), cell density was determined in different regions of the suture. Five different suture zones were chosen, as follows: 1) the midpalatal suture area in the 1st molar tooth region, 2) the midpalatal suture area between the 1st and 2nd molar teeth and between the 2nd molars, 3) the transverse palatine suture area between the 2nd molar teeth and between the 2nd and 3rd molar teeth, 4) the area between 2nd and 3rd molar teeth and the 3rd molar teeth, and 5) the area between the 3rd molar teeth and the interpalatine suture in the posterior region of the palate. The number of cells was determined in the

total area of each palatal suture zone (shown in Fig. 2) by counting the number of cell nuclei in the midpalatal area. The final statistical analysis of cell density was based on the number of cells in a 100- $\mu\text{m}^2$  suture area of each palatal suture zone.

#### Histochemistry and immunofluorescence labeling

For apoptosis detection, *In Situ* Cell Death Detection kit, Fluorescein TUNEL system (Roche Diagnostics, Mannheim, Germany), was used to visualize apoptotic cells.

Safranin O/Methyl Green staining was used to visualize cartilage proteoglycans and bone in frozen sections. Briefly, frozen sections were fixed overnight in 4% (w/v) paraformaldehyde in PBS, demineralized in 0.5 M EDTA for 14 days at 4°C, and embedded in Tissue-Tek OCT compound (Sakura Finetek USA, Inc., Torrance, CA, USA) with a slurry of solid CO<sub>2</sub> in 95% ethanol. Frozen blocks were sectioned using Leica cryotome (Research Cryostat Leica CM3050 S; Leica Microsystems Inc., Buffalo Grove, IL, USA) and air-dried for 30 min. The 8- $\mu\text{m}$  sections were visualized using a fluorescence microscope (Nikon TE2000 w/C1 Point Scanning Confocal; Japan).

For collagen types I and II immunohistochemistry, paraffin sections were deparaffinized and pre-washed prior to enzyme treatments. The tissue sections were digested by sequential treatment with 2 mg/ml of hyaluronidase (Sigma-Aldrich, St. Louis, MO, USA) in PBS (pH 5.0) for 15 min at 37°C; 250 mU/ml of chondroitinase ABC (Sigma-Aldrich) in 50 mM Tris, PH 8.0, 60 mM sodium acetate, and 0.02% bovine serum albumin (prepared fresh) for 15 min at 37°C; and finally pepsin (Sigma-Aldrich) at 2 mg/ml in 0.1 M Tris-HCl, pH 2.0 for 15 min at 37°C. After enzyme pre-treatments, sections were incubated separately with rabbit polyclonal antibody (Abcam, Cambridge, MA, USA) against collagen type I at 1:100 dilution and mouse monoclonal antibody (Lab Vision, Fremont, CA, USA) against collagen type II at 1:100 dilution overnight. MOM kit (Vector Laboratories, Burlingame, CA, USA) was used to decrease the background staining. Each experimental group consisted of a minimum of four mice with four sections per mouse.

#### Statistical analysis

Results were presented as mean  $\pm$  SD. Cell count differences were compared using two-tailed unpaired Student's *t* test ( $p < 0.05$ ).

## Results

Hematoxylin- and eosin-stained transverse sections of 6-week-old mouse hard palate (Fig. 1A–D) show the presence of three sutures: 1) midpalatal suture (mps) in the middle with a straight shape which narrows down at both poles (Fig. 1A, B), 2) transverse palatine suture (tps) formed as an interlocking joint with a highly complex interdigitated structure (Fig. 1A, C), and 3) interpalatine suture (ips) with an irregular zigzag shape at the posterior end (Fig. 1A, D). Nasal-associated lymphoid tissue (NALT) is prominent between the left and right lateral nasal glands (LNG). The 1st, 2nd, and 3rd molar teeth are seen along the sides of the palate. The bones that meet in midpalatal suture, known as the palatine process of maxilla (ppm), meet in a butt joint. The two halves of the horizontal plates of the palatine bones (p) are joined in the middle at the interpalatine suture and form the posterior section of the hard palate. The occlusal views of the reconstructed hard palate in two- and three-dimensional micro-CT images further confirm the histological findings (Fig. 1E, F).

The amount of bone marrow in the bony elements close to the sutures varies in a characteristic fashion. In the midpalatal suture region of the hard palate, bone marrow space is much smaller than in the interpalatine suture area (Fig. 1A, E). This can be clearly seen in frontal sections of the reconstructed micro-CT image of the 6-week-old mouse palate (Fig. 2A1–A5). The small amount of bone marrow close to the transverse suture is similar to that of the midpalatal suture area.

Further histological examination of the midpalatal suture revealed that it mainly consists of secondary cartilage close to the bony edges and with a small amount of fibrous tissue in the central area. From the middle of the sutural gap, a lateral progression of small-sized cells to mature

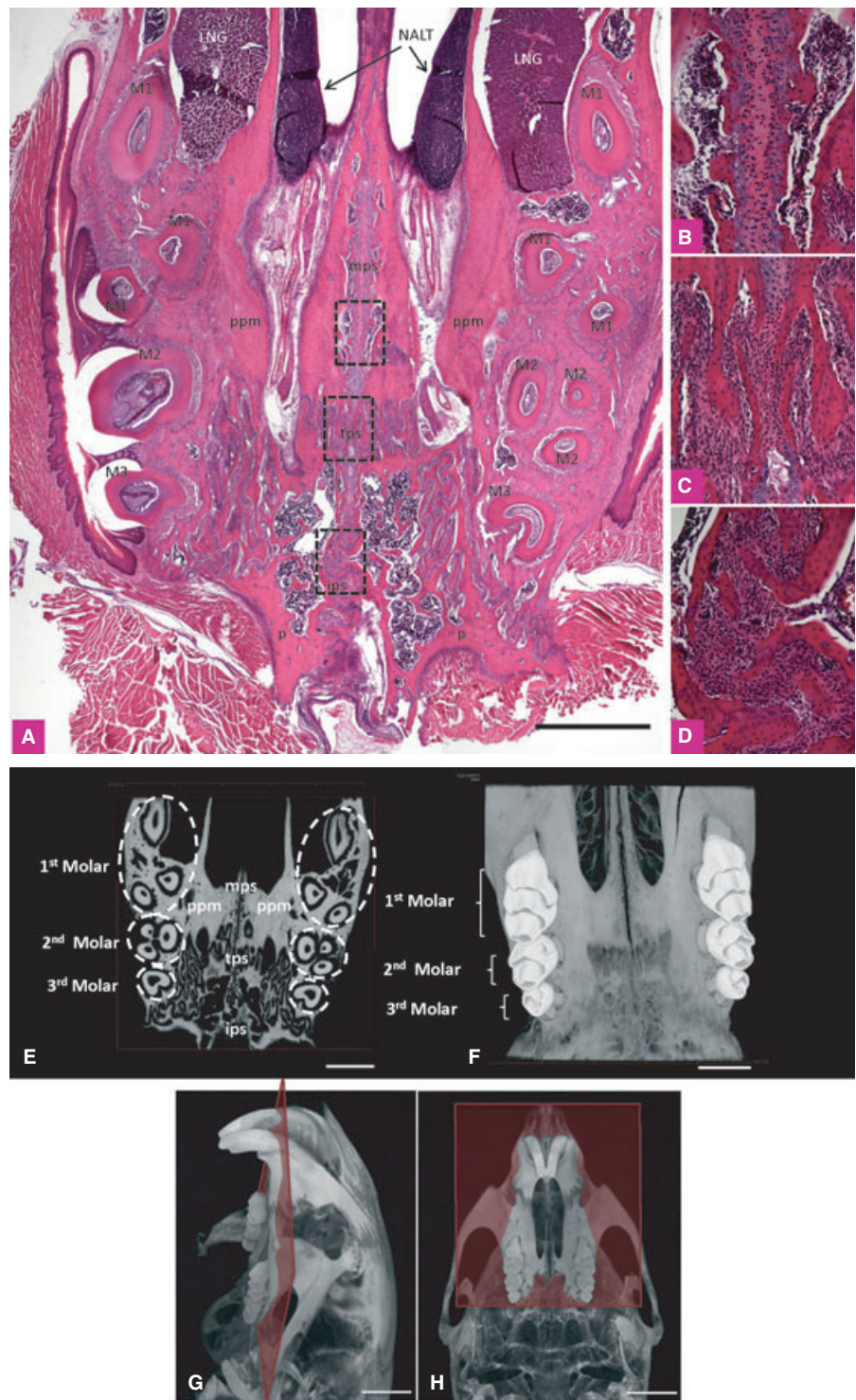


*Fig. 1.* A transverse section of mouse palate. Hematoxylin and eosin staining of 6-week-old mouse palate (A) with areas of the sutures as indicated by rectangles shown in higher magnification for the midpalatal suture (B), transverse suture (C), and interpalatine suture (D). A micro-CT image of 6-week-old male mouse palate reconstructed in two-dimensional (E) and three-dimensional (F–H) views. The transversal plane is indicated in the mouse palate (G–H) (NALT, nasal-associated lymphoid tissue; LNG, lateral nasal gland; M1, 1st molar; M2, 2nd molar; M3, 3rd molar; mps, midpalatal suture; tps, transverse palatine suture; ips, interpalatine suture; p, palatine bone; ppm, palatine process of maxilla). Scale bar (A, E, F): 1000  $\mu$ m.

chondrocytes and hypertrophic chondrocytes is evident.

The density of cells is notably variable between the different sutures. The posterior part of the hard palate shows the highest density of cells in both the transverse palatine suture and the interpalatine suture in comparison with the

midpalatal suture. This was confirmed by morphometric analysis based on examining histological sections (Fig. 2G) as described below.

To study the processes underlying age-related developmental changes in palatal sutures, a series of 6-week-old (Fig. 2B), 4- (Fig. 2C), 9- (Fig. 2D), and 12-month-old mice (Fig. 2E) were used. For

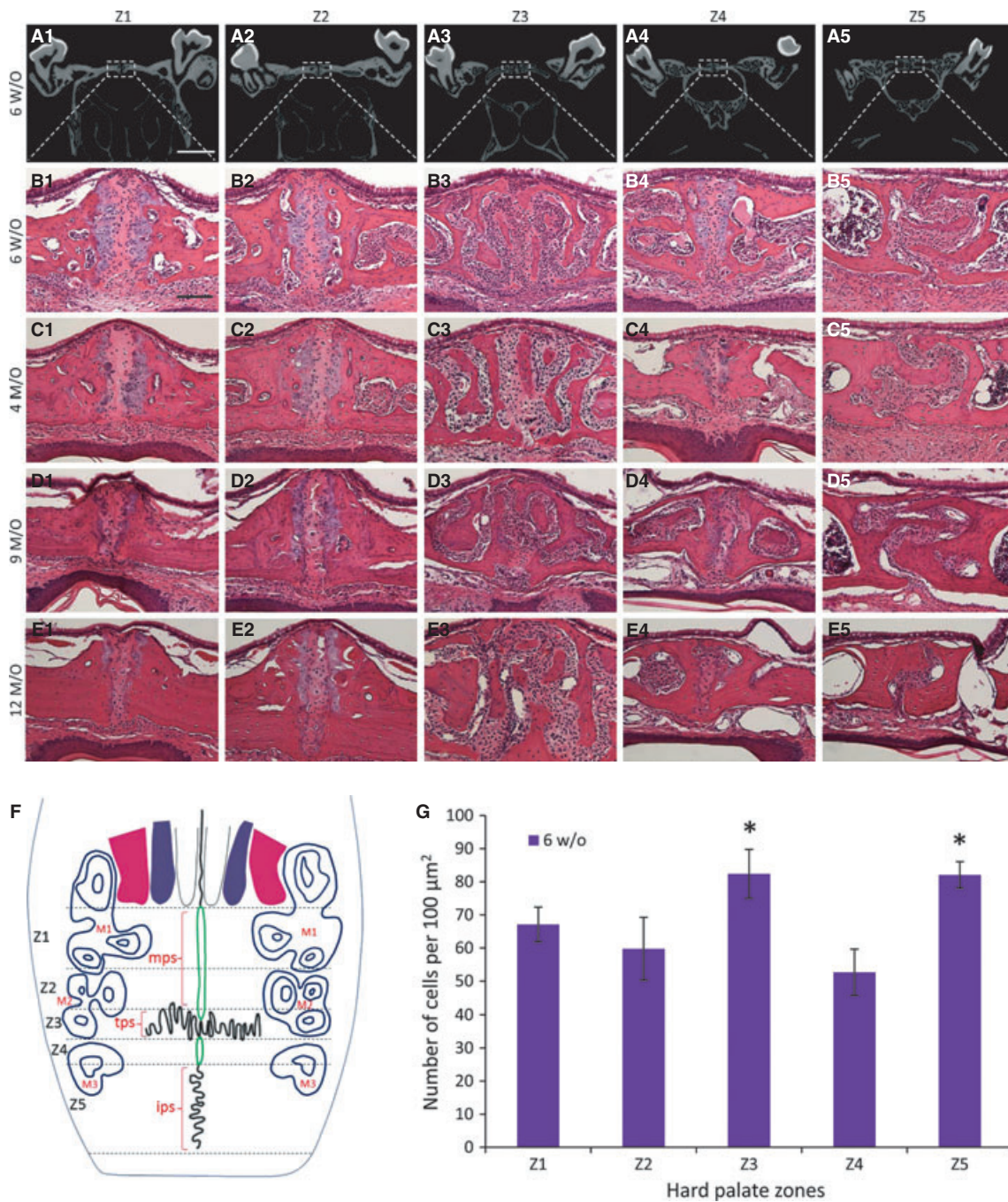


**Fig. 2.** Frontal section of mouse palate with the nasal side up and oral side down. Micro-CT reconstruction of frontal sections of 6-week-old male mouse palate in two-dimensional view (A1–A5) and stained with hematoxylin and eosin at different ages of 6-week-old (B1–B5), 4-month-old (C1–C5), 9-month-old (D1–D5), and 12-month-old (E1–E5) mice is shown. The panels are the representative of a series of sections of the palate divided into five different zones (F). Starting from the anterior aspect, these zones are [Z1] the suture between the 1st molar teeth (A1–E1), [Z2] the suture between 1st and the 2nd molar teeth and between the 2nd molars (A2–E2), [Z3] the transverse palatine suture between the 2nd molars and between the 2nd and the 3rd molars (A3–E3), [Z4] the zone between the 2nd and 3rd molars and between the 3rd molars (A4–E4), and [Z5] the zone between the 3rd molars and the interpalatine suture in the posterior part of the palate (A5–E5). The graph (G) represents the cell density in each designated zone of cut sections shown from panels 1–5 of series B (6-week-old mice). The cell density among Z1, Z2, and Z4 zones of midpalatal suture area was not significantly different. However, the cell density in midpalatal suture area was significantly lower in comparison with transverse palatine suture and/or the interpalatine suture ( $*p < 0.05$ ). Scale bar (A1): 1000  $\mu\text{m}$ , (B1): 100  $\mu\text{m}$ .

the comparison of suture morphology, the palate was divided into five different zones. Starting from the anterior aspect, these zones were 1) the suture

between the 1st molar teeth, 2) the suture between 1st and the 2nd molar teeth and between the 2nd molars, 3) the transverse palatine suture

between the 2nd molars and between the 2nd and the 3rd molars, 4) the zone between the 2nd and 3rd molars and between the 3rd molars, and 5) the zone between the 3rd molars and the interpalatine suture in the posterior part of the palate (Fig. 2A–F). The most obvious changes because of increasing age were decreasing bone marrow spaces in the surrounding bones, a reduced number of chondrocytes, a decreasing amount of fibrous tissue between the two cartilaginous regions along the bone margins, a reducing number of periosteal cells in oral and nasal sides, and increased bone formation. Accordingly, the age-dependent progressive ossification in the interdigitated area of the transverse palatal suture results in a more complex structure (Fig. 2B3–E3). In contrast, the midpalatal suture did not ossify during the ages analyzed here.

To determine whether the density of cells varied among the different types of sutures, cell nuclei were counted in the five different suture zones in 6-week-old control mice. The data show that there is a significant difference in the cell number per unit area ( $100 \mu\text{m}^2$ ) among the different suture types. The cell density in the transverse palatine

suture and the interpalatine suture was significantly higher than in the midpalatal suture area (Fig. 2G).

In response to expansive force, the width of the midpalatal suture increased (Fig. 3C). After 2 days of expansion, an increased amount of fibrous tissue and a decrease in the number of chondrocytes was observed. No difference was detected between sham-operated and non-operated mice. Accordingly, these two groups of animals were grouped together as controls. The changes occurring as a result of suture expansion have been previously published (4). Briefly, the collagen fibers are reoriented across the suture, and periosteal cells migrate into the suture area. Analysis of suture cell counts per unit area ( $100 \mu\text{m}^2$ ) shows that the cell density is significantly lower in the zones 1–4 of the expanded suture of 6-week-old mice than in control mice of the same age (Fig. 3D). This is primarily the result of expansion of the suture area, although apoptosis, induced by the expansion, contributes as well. The cell number per unit area in zone 5 of expanded palate (interpalatine suture) was lower, but not significant, in comparison with the

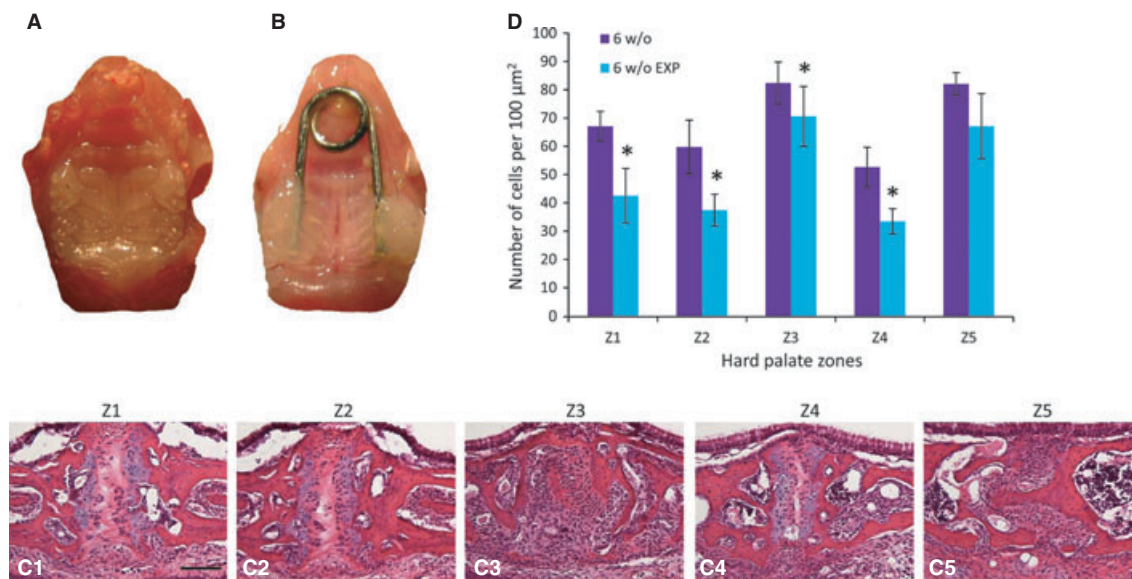


Fig. 3. Midpalatal suture expansion in mouse. Isolated palate of 6-week-old mice is shown with the spring opening loop bonded to the first and second molars (B) vs. the non-operated control (A). Hematoxylin and eosin staining of sections of expanded palate of 6-week-old mouse with sections representing the palate divided into five different zones. Starting from the anterior aspect, these zones are [Z1] the suture between the 1st molar teeth (C1), [Z2] the suture between 1st and the 2nd molar teeth and between the 2nd molars (C2), [Z3] the transverse palatine suture between the 2nd molars and between the 2nd and the 3rd molars (C3), [Z4] the zone between the 2nd and 3rd molars and between the 3rd molars (C4), and [Z5] the zone between the 3rd molars and the interpalatine suture in the posterior part of the palate (C5). The cell density of expanded palate in zones 1 through 5 of 6-week-old mice compared with same age non-operated control mice (D) was significantly lower ( $*p < 0.05$ ). Scale bar (C1):  $100 \mu\text{m}$ .

control group. This may be due to the fact that the interpalatine suture is less affected by the process of midpalatal suture expansion.

To further evaluate and explain the reasons behind the decreased cell density in the midpalatal suture-expanded mice, TUNEL staining for apoptosis of control and expanded midpalatal sutures was performed. Cell proliferation, differentiation, and apoptosis are the key events that occur during tissue remodeling. In control mice, TUNEL-positive cells were mainly seen in the cartilaginous region. In contrast, in the expansion group of mice, TUNEL-positive cells were detected in both periosteal and cartilaginous regions (Fig. 4A–C). Using Safranin O staining, we found that the application of force across the midpalatal suture caused a decrease in the amount of secondary cartilage (Fig. 5). The significant loss of proteoglycan as judged by decreased Safranin O staining suggests that the tensile force across the suture may induce release and/or activation of matrix-degrading proteases in the suture (Fig. 5B). Finally, collagen I- and II-specific immunofluorescence staining of midpalatal and transverse palatine sutures was conducted. First, analysis of the control group showed that there was an expression of both types of collagen in the midpalatal suture area (Fig. 6A1–A2); further down from the midpalatal area, in the transverse

palatine suture, only collagen I staining was detected (Fig. 7A). Of note, the bone matrix in the palatal shelves and periosteal cells on both the oral and nasal sides were clearly stained by collagen I antibodies (Figs 6 and 7). Second, analysis of the stretched collagen fibers in the midpalatal suture of the expansion group showed mainly the expression of collagen II (Fig. 6B2); however, the matrix surrounding some of the mesenchymal cells in the middle of midpalatal suture area showed the expression of collagen I (Fig. 6B1). In accordance with the results for the control group (Fig. 7A), there was no collagen II expression in the transverse palatine suture of the expansion group; only collagen I was detected (Fig. 7B). The stretched collagen fibers in the transverse palatine area were also stained only with collagen I antibodies (Fig. 7B). Overall, this suggests that the midpalatal suture in mice is more like a fibrocartilage growth region than a collagen I-based fibrous connection between the palatal bones, whereas the transverse palatine area is more like a fibrous suture.

## Discussion

The aims of the present study were to investigate the anatomy of the mouse palate at different ages,

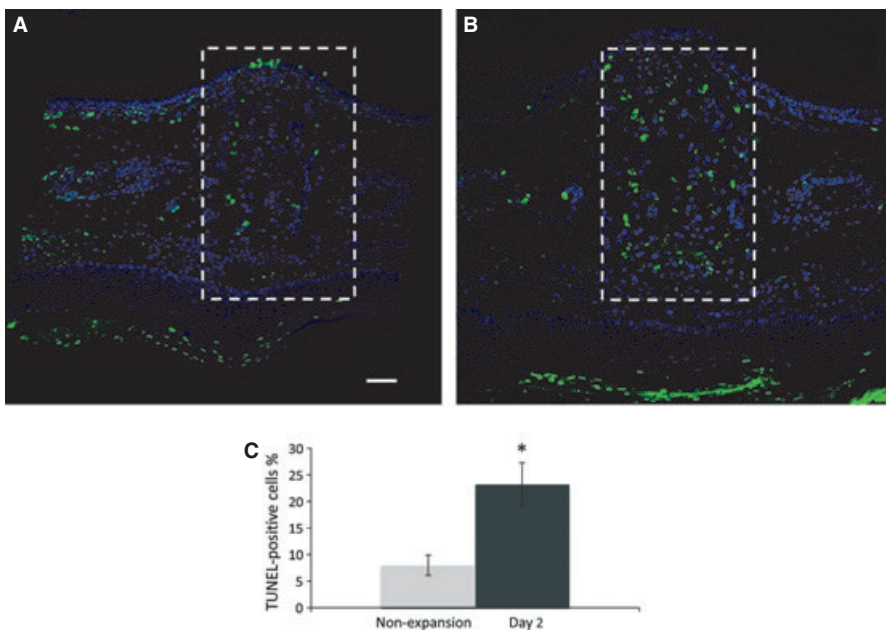


*Fig. 4.* Increased apoptosis of chondrocytes in expanded midpalatal suture. TUNEL staining of non-operated control (A) and expanded midpalatal suture (B) of 6-week-old mice. After 2 days of midpalatal suture expansion, TUNEL-positive cells (green) were detected in the regions of periosteal cells and chondrocytes within the midpalatal suture area. The percentage of TUNEL-positive cells among the total cells within the midpalatal suture area is compared between control and expansion groups (\* $p < 0.05$ ) (C). Scale bar: (A) 100  $\mu\text{m}$ .

Fig. 5. Safranin O/Methyl Green staining of non-operated control (A) and expanded midpalatal suture (B) of 6-week-old mouse at day 2 of expansion. Scale bar (A): 100  $\mu$ m.

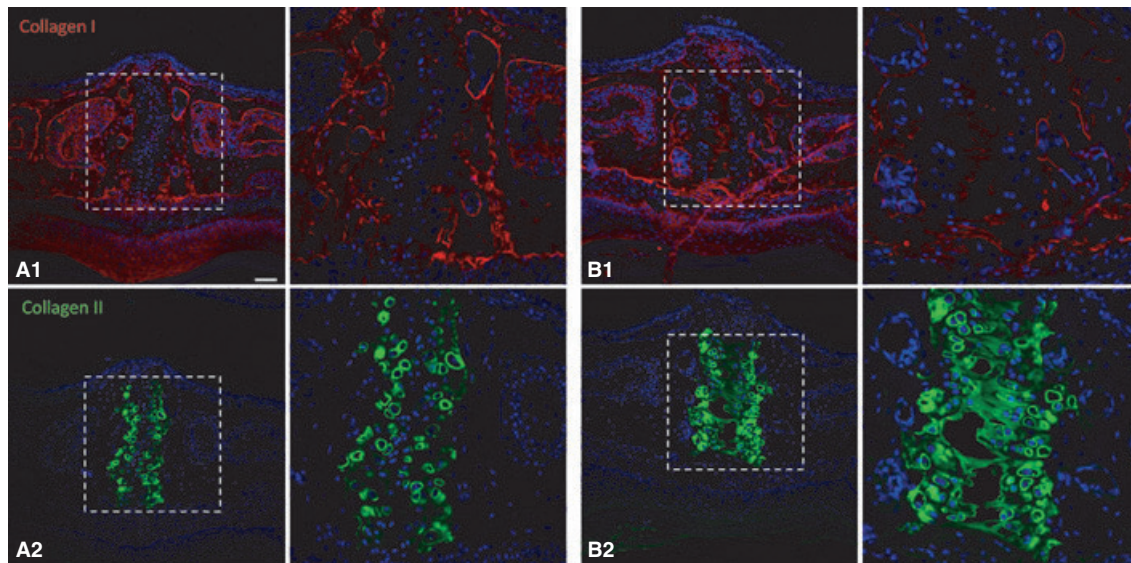
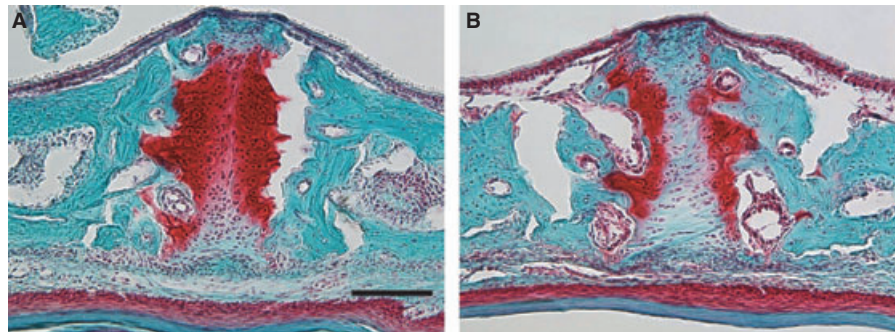


Fig. 6. Confocal images of immunofluorescence staining for collagen types I (red) and II (green) of serial palatal sections of non-operated control (A) and expanded midpalatal sutures (B) of 6-week-old mice. After 2 days of midpalatal suture expansion, the stretched collagen fibers in the midpalatal suture area were mostly stained with collagen II-specific antibody. Scale bar (A): 100  $\mu$ m.

compare morphological features of the midpalatal suture before and right after mechanical stimuli, and study cellular changes resulting from midpalatal suture expansion. The study documents that the midpalatal suture in mice mainly consists of secondary cartilage with collagen II-rich fibrous connective tissue in the central area between two cartilaginous regions.

As in many other anatomical aspects in mice and humans, the palatal structure of the two species shows similarities. Both human and mouse osseous palates consist of the horizontal processes of the palatine bone posterior to the transverse palatine suture and the palatine processes of the maxillary bone anterior to that suture. Both bones are joined by sutures that are arranged in two anatomical planes, the transverse and sagittal. This structure allows the palate to

grow in two directions, elongate in the antero-posterior direction and widen in the lateral direction (2, 5). While the trigger for widening growth originates from inside the sagittal midpalatal and interpalatine sutures, the transverse palatine suture functions as a growth center for anteroposterior elongation (6).

While mice and humans share similarities in the anatomy of palatal sutures, there are some notable differences. Palatal growth and suture morphology in humans were investigated by Melsen from birth to adulthood (7). Three stages were shown in the Melsen study: in the infantile period, the suture was broad and Y-shaped; in the juvenile period, the suture was longer in the vertical aspect and started to become interdigitated; and finally, in the adolescent stage, the suture was very tortuous with increased interdigitation. (7).

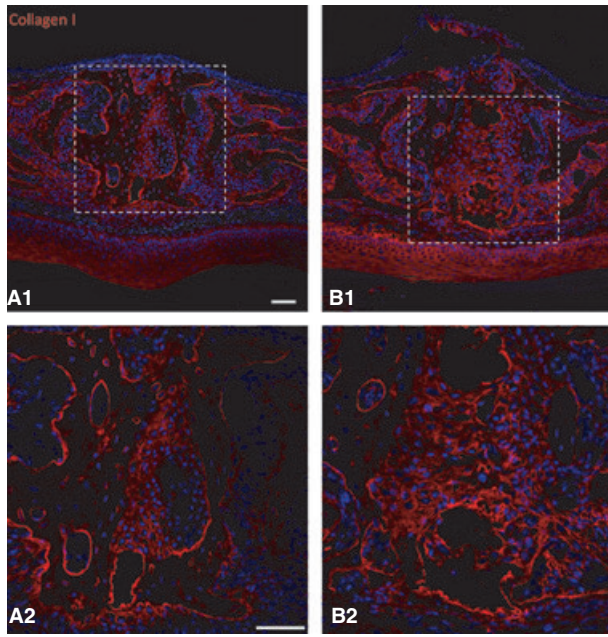


**Fig. 7.** The collagen I-specific immunofluorescence staining of non-operated control (A) and expanded transverse palatine sutures (B) of 6-week-old mice. The transverse palatine suture area was only stained with collagen I-specific antibody in both the non-operated and expansion groups. Scale bar (A1, A2): 100  $\mu\text{m}$ .

However, the midpalatal suture in adult mice is a straight line between the palatal bones, while in humans it forms an interdigitated structure. Another difference is the presence of secondary cartilage in the mouse and the absence of it in humans. Previous studies in rodents have shown that secondary cartilage only forms in response to mechanical stimulation (8, 9). It has also been reported that the type of stimulation makes a significant difference in the outcome. While mechanical tension combined with hyperoxia can boost mesenchymal cell differentiation into osteoblasts, mechanical stress combined with ischemia and hypoxia can favor differentiation into chondroblasts (10, 11). Another factor that can affect the development of sutural cartilage is the masticatory forces that are quite different between mice and humans (12). Accordingly, changes in various forces during craniofacial growth and development, and differences in the masticatory forces, dentition, and occlusion between mice and humans, are likely among the reasons for the presence of secondary cartilage in mice and the absence of it in humans.

In mammals, the sutures are considered to be fibrocellular tissues which are adapted to various types of strain that are different in pattern and magnitude (1). In children and youngsters with cases of transverse maxillary hypoplasia, rapid maxillary expansion (RME) is chosen as a treatment option (3, 13). When RME is performed in the human palate, the opening of the midpalatal suture is not the only effect. In fact, the circumaxillary sutures separating maxilla from adjacent facial bones are also affected (14). As a result, they show bony displacement responses that are highly variable among sutures (15). Different structures of the skull, including the nasal septum, experience various stresses applied during midpalatal suture expansion (16). As previously described, the study of *Wnt1Cre;Pkd1* mice showed that the nasal cartilage, one of the surrounding areas of the midpalatal suture, experienced abnormal ossification during postnatal development and in response to midpalatal suture expansion (17). In our present study, both transverse and interpalatine sutures are also seen to be affected during midpalatal suture expansion. The decreased cell density in different types of sutures of the expansion group vs. the control group of mice is likely a consequence of the diverse effects of the midpalatal suture expansion procedure. These effects are likely to be more absorbed by the midpalatal area than by the interpalatine suture area. Although the density of mesenchymal cells in the interpalatine suture of expansion mice was slightly lower in comparison with the control group, the difference was not statistically significant. This is an indication of the smaller effect of midpalatal suture expansion on the posterior hard palate. In addition, the apoptosis measurements showed an increased number of TUNEL-positive cells in the midpalatal suture area. However, differences in cellular density are not only based on the role of apoptosis of cells but also correlated with the size of the matrix space. As the matrix area increases because of the expansion, some of the cells die, while the remaining cells are scattered around. As a result, the density of cells in the midpalatal suture area decreases. On the other hand, the decreased density of mesenchymal cells in the transverse

palatine and interpalatine sutures is mainly because of the dispersion of cells owing to the force-induced increase in the suture matrix space.

The spheno-occipital synchondrosis plays a major role in growth of the cranial base (18). In the study of Cendekiawan et al. (19), it was shown that mechanical tension stimuli increased the expression of collagen type II in the spheno-occipital synchondrosis of mice (19). Thus, we speculate that the collagen type II expression in the expanded midpalatal suture of mice may be the result of stretching the suture tissue. Additionally, the collagen I expression in the matrix surrounding mesenchymal cells residing in the expanded midpalatal suture area may be an indication that these cells are differentiating osteoblasts. Such collagen I-expressing cells were also found among the periosteal cells on both the oral and nasal sides of the suture.

## Conclusion

This study suggests that the midpalatal suture in mice is more like a fibro-cartilage growth region than a collagen I-based fibrous connection between the palatal bones. In contrast, the transverse palatine area is more like a fibrous suture. Furthermore, we described the morphological and histological properties of the

mouse midpalatal suture in detail. This will serve as the basis for further studies of the molecular and cellular mechanisms involved in suture development and responses to mechanical manipulation. Understanding these mechanisms will be required for improving the clinical outcomes of orthopedic–orthodontic therapies in human patients.

## Clinical relevance

There are notable similarities and differences in the anatomy of palatal sutures between mice and humans. For half a century, the midpalatal suture expansion technique has been widely used to correct dentofacial deformities and treat maxillary width deficiencies in humans. However, the cellular and molecular mechanisms underlying the responses of suture tissue to mechanical forces have not been fully understood. This study provides the basis for the experimental work in mice that will be needed for improving the clinical outcomes of orthopedic–orthodontic therapies in human patients.

**Acknowledgements:** We would like to thank the Nikon Imaging Center at Harvard Medical School. This work was supported by research grant R01AR036819 from the National Institutes of Health (to B.R.O.).

## References

- Herring SW. Mechanical influences on suture development and patency. *Front Oral Biol* 2008;12:41–56.
- Yu HS, Baike HS, Sung SJ, Kim KD, Cho YS. Three-dimensional finite-element analysis of maxillary protrusion with and without rapid palatal expansion. *Euro J of Orthod* 2007;29:118–25.
- Haas AJ. Rapid expansion of the maxillary dental arch and nasal cavity by opening the midpalatal suture. *Angle Orthod* 1961;31:73–90.
- Hou B, Fukai N, Olsen BR. Mechanical force-induced midpalatal suture remodeling in mice. *Bone* 2007;40:1483–93.
- Raisz LG. Physiology and pathophysiology of bone remodeling. *Clin Chem* 1999;45:1353–8.
- Silau AM, Nijo B, Solow B, Kjaer I. Prenatal sagittal growth of the osseous components of the human palate. *J Craniofac Gen Dev Biol* 1994;14:252–6.
- Melsen B. Palatal growth studied on human autopsy material. *Am J Orthod* 1970;68:42–54.
- Yu JC, Wright R, Williamson MA, Braselton JP, Abell ML. A fractal analysis of human cranial sutures. *Cleft Pal-Craniofac J* 2003;40:409–15.
- Alaqeel SM, Hinton RJ, Opperman LA. Cellular response to force application at craniofacial sutures. *Orthod Craniofac Res* 2006;9:111–22.
- Hall BK. Cellular differentiation in skeletal tissues. *Biol RevCamb Philos Soc* 1970;45:455–84.
- Rice DP. Developmental anatomy of craniofacial sutures. In: Rice DP, editor. *Craniofacial Sutures. Development, Disease and Treatment. Front Oral Biol*. Basel: Karger; 2008;12:1–21.
- Hinton RJ. Response of the intermaxillary suture cartilage to alterations in masticatory function. *Anat Rec* 1988;220:376–87.
- Suri L, Taneja P. Surgically assisted rapid palatal expansion: a literature review. *Am J Orthod Dentofacial Orthop* 2008;133:290–302.
- Leonardi R, Sicurezza E, Cutrera A, Barbato E. Early post-treatment changes of circumaxillary sutures in young patients treated with rapid

- maxillary expansion. *Angle Orthod* 2011;81:36–41.
15. Sun A, Hueni S, Tee BC, Kim H. Mechanical strain at alveolar bone and circummaxillary sutures during acute rapid palatal expansion. *Am J Orthod Dentofacial Orthop* 2011;139:219–28.
  16. Jafari A, Shetty KS, Kumar M. Study of stress distribution and displacement of various craniofacial structures following application of transverse orthopedic forces—a three-dimensional FEM study. *Angle Orthod* 2003;73:12–20.
  17. Hou B, Kolpakova-Hart E, Fukai N, Wu K, Olsen BR. The polycystic kidney disease 1 (Pkd1) gene is required for the responses of osteochondroprogenitor cells to midpalatal suture expansion in mice. *Bone* 2009;44:1121–33.
  18. Tang M, Mao JJ. Matrix and gene expression in the rat cranial base growth plate. *Cell Tissue Res* 2006;324:467–74.
  19. Cendekiawan T, Wong RW, Rabie AB. Temporal expression of SOX9 and type II collagen in spheno-occipital synchondrosis of mice after mechanical tension stimuli. *Angle Orthod* 2008;78:83–8.

Copyright of Orthodontics & Craniofacial Research is the property of Wiley-Blackwell and its content may not be copied or emailed to multiple sites or posted to a listserv without the copyright holder's express written permission. However, users may print, download, or email articles for individual use.